Echocardiographic Evaluation of the Etiology and Mechanism of Native Aortic Valve Regurgitation

David T. Harnett, MD, Ibrahim Jelaidan, MBBS, Munir Boodhwani, MD, Ian G. Burwash, MD, Kwan-Leung Chan, MD, Thais Coutinho, MD, Alain Berrebi, MD, Jean-Louis Vanoverschelde, MD, PhD, David Messika-Zeitoun, MD, PhD, and Luc Beauchesne, MD, *Ottawa, Ontario, Canada; Paris, France; and Brussels, Belgium*

INTRODUCTION

There has been a growing trend toward increasing utilization of aortic valve–sparing surgical procedures for treating aortic regurgitation (AR). Understanding the mechanism of AR informs the surgical approach, a concept that led to the development of a repair-oriented functional classification by El Khoury, inspired from Carpentier's classification of mitral regurgitation.[1,2] While it may be possible in some patients to accurately classify the mechanism of AR by transthoracic echocardiography (TTE), the majority of the literature is based on transesophageal echocardiography (TEE).[3,4]

A working understanding of the anatomy of the aortic valve and surrounding structures is a prerequisite for approaching the echocardiographic assessment of AR. Comprehensive reviews of aortic valve anatomy have been previously published, with basic concepts summarized in Figure 1.[5] An important concept is that pathology involving either the aortic cusps or surrounding aortic structures can lead to AR. In the El Khoury classification, type Ia-Ic lesions are due to enlargement of the functional aortic annulus (FAA) with normal leaflet motion, whereas type Id is reserved for cases of cusp perforation. Type II lesions involve excessive cusp motion resulting in cusp prolapse. Type III lesions indicate restricted cusp motion from calcific degeneration or fibrosis.[2]

We present a series of cases that illustrate the process of defining AR mechanisms that will enable echocardiographers to communicate with surgeons in a common language (Figures 1-7, Videos 1-6). For illustrative purposes, these cases tend to involve one mechanism, but it is important to note that multiple mechanisms frequently coexist.[1] While the examples we present involve tricuspid aortic valves, the classification system can also be applied to bicuspid valves.

CASE PRESENTATION

Case 1

A 65-year-old woman was referred to the echocardiography laboratory to rule out left ventricular (LV) hypertrophy in the setting of systemic hypertension. She denied cardiovascular symptoms. On exam, there was a wide pulse pressure (150/72 mm Hg). Heart rate was 72 bpm. No diastolic murmur could be heard, which may have been due to the patient's challenging body habitus. She underwent a TTE, which revealed a trileaflet aortic valve and moderate central AR (vena contracta width [VCW] = 0.5 cm, jet width ratio [JWR] = 41%) due to severe ascending aorta enlargement (6.5 cm) extending to the sinotubular junction (STJ; 5.0 cm). The aortic root (3.2 cm) and annulus (2.0 cm) size were normal (Figure 2, Video 1). Her LV end-diastolic diameter (LVEDD) was 5.7 cm; LV end-systolic diameter (LVESD), 3.1 cm; and LV ejection fraction (LVEF), 76% (Teichholz). She underwent valve-sparing replacement of the ascending aorta with aortic valve repair. Pathology revealed lymphoplasmacytic aortitis. Subsequently, the patient was assessed by the rheumatology service and found to have visual symptomatology and an elevated erythrocyte sedimentation rate (46 mm/hour). A temporal artery biopsy confirmed the presence of giant cell arteritis. Type Ia AR refers to distal ascending aorta enlargement including the STJ with normal aortic root size. Enlargement of the FAA can lead to failure of central coaptation resulting typically in a central jet of AR. An eccentric jet in a patient with a type I lesion should prompt suspicion for a coexisting type II pathology or may reflect asymmetric FAA enlargement. Isolated dilatation of the distal ascending aorta without involvement of the STJ is not felt to be a contributor to AR.

Case 2

A 60-year-old man was referred to the out-patient clinic for evaluation of New York Heart Association (NYHA) class II dyspnea. On exam there was a class III/IV diastolic murmur. Blood pressure was 140/70 mm Hg, and heart rate was 100 bpm. A TEE identified a trileaflet aortic valve and severe aortic root enlargement (6.5 cm) resulting in a central coaptation defect and jet of severe AR (VCW = 0.7 cm, JWR = 65%; Figure 3, Video 2). The aortic annulus (AoA; 2.7 cm), STJ (6.2 cm), and ascending aorta (4.6 cm) were also enlarged. His LVEDD was 7.1 cm; LVESD, 6.4 cm; and LVEF, 40% (Simpson's). He underwent aortic root replacement and bioprosthetic aortic valve replacement with surgical pathology showing severe medial degeneration of the aorta, which is classically, although not exclusively,

From the Department of Medicine, Division of Cardiology (D.T.H., I.J., I.G.B., K.-L.C., T.C., D.M.-Z., L.B.), Division of Cardiac Surgery (M.B.), and Division of Cardiac Prevention and Rehabilitation (T.C.), University of Ottawa Heart Institute, Ottawa, Ontario, Canada; Division of Cardiology, Institut Mutualiste Montsouris (A.B.), Paris, France; and Division of Cardiology, Cliniques Universitaires St-Luc, Catholic (J.-L.V.), Brussels, Belgium.

Keywords: Aortic regurgitation, Echocardiography

Conflicts of interest: The authors reported no actual or potential conflicts of interest relative to this document.

Correspondence: Luc Beauchesne, MD, Division of Cardiology, University of Ottawa Heart Institute, 40 Ruskin Street, Ottawa, Ontario K1Y 4W7. (E-mail: *lbeauchesne@ottawaheart.ca*).

2468-6441

https://doi.org/10.1016/j.case.2022.03.004

VIDEO HIGHLIGHTS

Video 1: Type 1a AR. Composite clip consisting of a 2D parasternal long-axis TTE view, followed by zoom with color, then TEE short-axis view of the aortic valve, then with color. The aortic valve is trileaflet with a central jet of moderate AR. The AR is due to severe enlargement of the ascending aorta (6.5 cm) extending to the STJ. The aortic root and annulus size are normal. Refer to Figure 2.

Video 2: Type 1b AR. Composite clip consisting of a 2D TEE long-axis view of the aortic valve with color compare, followed by TEE short-axis view of the aortic valve, then with color. Trileaflet aortic valve with severe aortic root enlargement (6.5 cm) resulting in a central coaptation defect associated with severe AR. The AoA (2.7 cm), STJ (6.2 cm), and ascending aorta (4.6 cm) were also enlarged. Refer to Figure 3.

Video 3: Type 1c AR. Composite clip consisting of a 2D TEE long-axis view of the trileaflet aortic valve, then zoomed view, then color, then short-axis of the aortic valve, then color. There is isolated dilatation of the AoA (3.0 cm) leading to severe AR. The aortic root, STJ, and ascending aorta were normal in size. Refer to Figure 4.

Video 4: Type 1d AR. Composite clip consisting of a 2D TEE midesophageal long-axis view, followed by zoom view of the trileaflet aortic valve with color compare, then short-axis zoom view of the aortic valve, then with color. There is a perforated diverticulum of the noncoronary cusp leading to severe AR. Refer to Figure 5.

Video 5: Type II AR. Composite clip consisting of a 2D TTE long-axis 2D zoom view of the trileaflet aortic valve, then with color, then short-axis view, then with color. There is prolapse of the right coronary cusp leading to eccentric severe AR. Refer to Figure 6.

Video 6: Type III AR. Composite clip consisting of 2D TEE zoom long-axis view, followed by color, then short-axis view of the aortic valve, then with color. The valve is trileaflet valve with moderate degenerative sclerosis and asymmetric restricted diastolic motion of the noncoronary cusp resulting in right coronary cusp coaptation below the level of the noncoronary cusp and an eccentric jet of severe AR. Refer to Figure 7.

View the video content online at www.cvcasejournal.com.

associated with connective tissue disorders.[7] This patient had no identifiable systemic disease. Type Ib pathology is seen with aortic root enlargement and generally leads to a central jet of AR unless the root enlargement is asymmetric or there is concurrent prolapse or intrinsic cusp restriction.

Case 3

A 29-year-old man with a history of anthracycline-induced cardiomyopathy who was followed at the heart function clinic underwent a TTE to monitor LV function. On exam he was euvolemic, and a class I/IV murmur could be heard on auscultation. His blood pressure was 122/58 mm Hg, and heart rate was 84 bpm. On the TTE, LVEDD was 6.3 cm; LVESD, 5.2 cm; and LVEF, 35% (Simpson's). Aortic regurgitation was detected, which was felt to be initially moderate in severity. A subsequent TEE demonstrated a trileaflet aortic valve and isolated enlargement of the AoA (3.0 cm) resulting in a central jet of severe AR (VCW = 0.8 cm, JWR = 61%; Figure 4, Video 3). The aortic root (3.5 cm), STJ (2.8 cm), and ascending aorta (3.0 cm) were within normal limits. Direct operative evaluation revealed normal cusp mobility with no degenerative abnormalities or alternate explanation for AR. Pathology revealed myxomatous changes of the leaflets. An initial attempt at valve repair resulted in moderate AR, so a mechanical prosthesis was placed. Rarely seen in isolation, but often coexisting with other mechanisms, type Ic lesions occur in cases of isolated enlargement of the AoA.

Case 4

On serial surveillance imaging, a 56-year-old man with a history of aortic valve enterococcus faecalis endocarditis with residual AR was found to have to progressive LV dilatation. He was asymptomatic. On exam he had collapsing peripheral pulses and a class III/IV diastolic murmur. His blood pressure was 120/60 mm Hg, and heart rate was 76 bpm. A TEE revealed a perforated diverticulum of the noncoronary cusp resulting in severe AR (VCW = 0.8 cm, JWR = 62%), confirming the etiology to be from the prior infective endocarditis (Figure 5, Video 4). The aortic root (4.3 cm) was mildly enlarged with normal size AoA (2.2 cm), STJ (3.5 cm), and ascending aorta (3.7 cm). His LVEDD was 6.4 cm; LVEDD, 4.5 cm; and LVEF, 56% (Teichholz). Type Id lesions include cases of cusp perforation from endocarditis, trauma, or other causes. In such cases, the jet of AR originates from a location outside the site of cusp coaptation. This highlights the point that pathology involving either the cusps or surrounding aortic structures can lead to AR.

Case 5

A 68-year-old man with known coronary artery disease was referred to the echocardiography laboratory for assessment of LV function. The patient was asymptomatic. On exam, there was a class II/IV diastolic murmur. His blood pressure was 114/58 mm Hg, and heart rate was 60 bpm. A TTE demonstrated a trileaflet aortic valve and prolapse of the right coronary cusp with an eccentric jet of severe AR (VCW = 0.7 cm, flow reversal in descending aorta) directed toward the anterior mitral valve leaflet (Figure 6, Video 5). The AoA (2.4 cm), aortic root (3.4 cm), STJ (3.0 cm), and ascending aorta (3.2 cm) were normal in size. His LVEDD was 5.6 cm; LVESD, 3.1 cm; and LVEF, 75% (Teichholz). The patient has not yet had intervention and is undergoing clinical and echocardiographic surveillance in the absence of symptoms or significant LV enlargement or systolic dysfunction. Type II pathology (i.e., prolapse) should be suspected in cases of eccentric jets. The jet should be directed away from the culprit cusp. Leaflet coaptation normally occurs above the level of the annulus, typically at the middle of the sinuses of Valsalva. Aortic valve prolapse refers to culprit cusp malcoaptation below the adjacent leaflet in diastole. The effective height of the affected cusp will typically be <9 mm.

Case 6

A 76-year-old man with NYHA class II-III dyspnea was found to have severe AR with mild aortic stenosis on TTE. On exam there was a class II/IV systolic ejection murmur and a class III/IV diastolic murmur. His

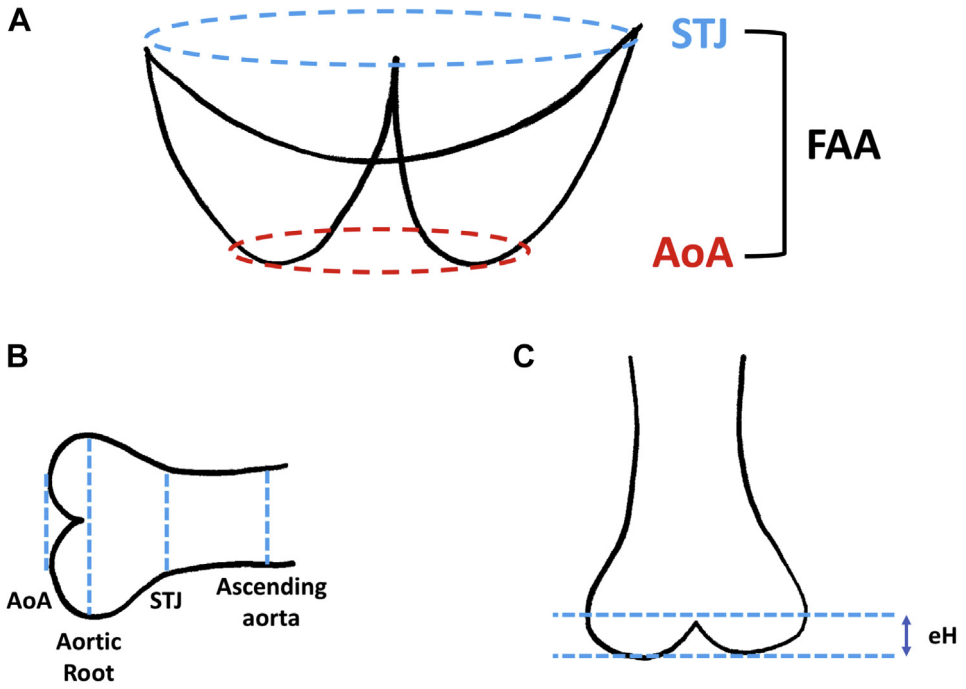

Figure 1 Basic anatomical concepts. **(A)** Within the functional aortic annulus (FAA), the cusps insert into the aortic wall in a semilunar fashion with the superior border at the STJ and inferior border at the aortic annulus (AoA). The AoA is best envisioned from an imaging perspective as a virtual plane joining the most basal portion or nadir of the aortic cusps (panel A is adapted from Piazza et al.[5]). Downstream to the AoA is the anatomic ventricular aortic junction, which is the transition area between the ventricular septum and the wall of the sinus of Valsalva (not illustrated in this diagram). **(B)** Components of the FAA should be measured at the different levels and dimensions compared with echocardiographic normal ranges.[6] The AoA is measured inner edge to inner edge from the leaflet insertion point in midsystole. In contrast, the aortic root and STJ are measured leading edge to leading edge at end diastole perpendicular to the long axis of the ascending aorta. **(C)** The effective height, measured as the orthogonal distance between the AoA and the central free margin of each cusp during diastole, is an important parameter in assessing cusp coaptation. Not well depicted in these images is the normal coaptation length at the tips of the cusps.

blood pressure was 159/68 mm Hg, and heart rate was 67 bpm. A TEE identified a trileaflet valve with moderate degenerative sclerosis and asymmetric restricted diastolic motion of the noncoronary cusp resulting in right coronary cusp coaptation below the level of the noncoronary cusp and an eccentric jet of severe AR (VCW = 0.6 cm and significant diastolic flow reversal seen in the descending aorta) directed toward the anterior mitral valve leaflet (Figure 7, Video 6). The Vmax was 2.7 cm/sec, and aortic valve area by planimetry was 1.9 cm^2. The ascending aorta (4.4 cm) was mildly enlarged with near normal AoA (2.6 cm), aortic root (3.7 cm), and STJ (3.7 cm) diameters. His LVEDD was 7.0 cm; LVESD, 5.7 cm; and LVEF, 40% (Simpson's). Type III lesions are seen with cusp restriction due to cusp thickening from calcific degeneration, rheumatic disease, or fibrosis. In cases of degenerative/rheumatic AR where all cusps are affected, the jet of AR should be central, whereas an eccentric jet would be expected in the event of asymmetric cusp thickening/restriction.

DISCUSSION

Echocardiography provides a dynamic assessment of both aortic valve anatomy and function. A systematic approach to the classification of the AR mechanism is an important step, in addition to the evaluation of AR severity. This approach aligns with the most recent American Society of Echocardiography guidelines on native valve regurgitation.[8] Adding to the complexity of classification is the frequent coexistence of more than one mechanism of AR. Previous cohorts of patients undergoing surgical intervention for AR have reported the presence of more than one mechanism in 36%-70% of patients, with the most frequent combination as types Ib and II.[1,9] Multiple mechanisms of AR appear more common in patients with a bicuspid aortic valve relative to those with trileaflet valves.[10] For illustrative purposes, we have provided a series of cases with one specific mechanism subtype in trileaflet valves, acknowledging that in reality there are additional complexities in many instances. Although aortic stenosis is usually the main hemodynamic problem in unicuspid aortic valves, the classification could be used in the minority of patients with a predominant regurgitant phenotype. However, the classification would be particularly useful in patients with quadricuspid valves as aortopathy and AR are common in this relatively rare congenital abnormality. Leaflet restriction is often part of the pathology of quadricuspid aortic valves. As bicuspid aortic valves are also frequently associated with significant aortopathy, the classification is once again particularly relevant as it emphasizes the role of the FAA in the surgical planning of these patients.

Intraoperative TEE is a critical tool to guide aortic valve repair where the expertise of the echocardiographer is relied upon to inform the suitability of repair, repair strategy, and postoperative outcome and has been comprehensively reviewed previously.[3,4,11] Comprehensive preoperative echocardiography, whether TTE or TEE, that fully explores the mechanism of AR can be of great value to the surgical and intraoperative echocardiography team. Transthoracic echocardiography can

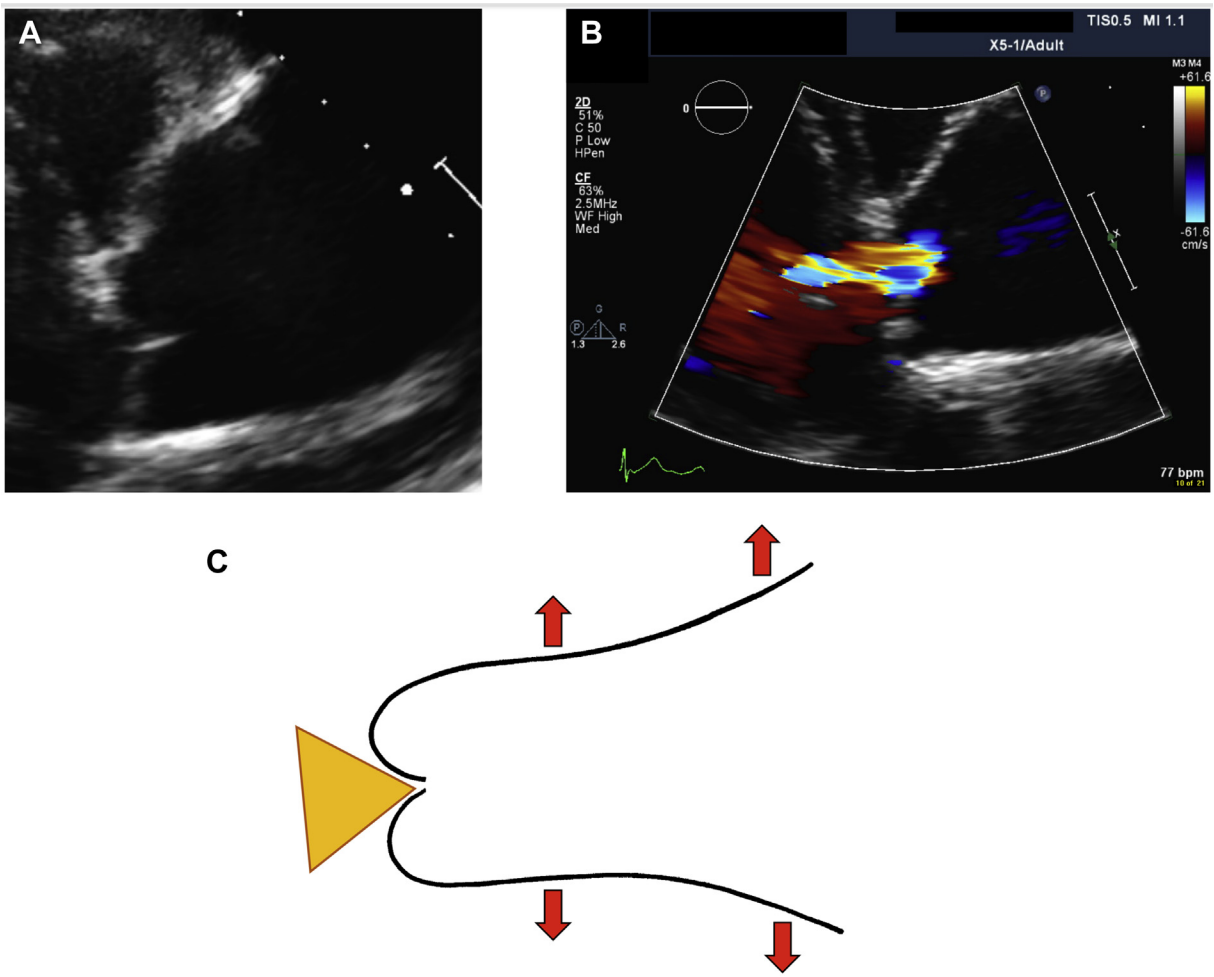

Figure 2 Type Ia AR. **(A, B)** Two-dimensional TTE parasternal long-axis view, diastolic phase, without and with color demonstrating moderate AR (Video 1). **(C)** Transthoracic echocardiographic long-axis view depiction showing distal ascending aorta enlargement including the STJ with normal aortic root size leading to a failure of central coaptation and a central jet of AR.

often provide a detailed description of the AR mechanism regarding aortic dimensions, the number of aortic cusps, the presence of degenerative abnormalities/calcification, and cusp mobility. Transesophageal echocardiography is generally reserved for patients who are planned for surgical intervention or in whom transthoracic acoustic windows are of poor quality or when there is uncertainty regarding the severity and/or mechanism of AR despite a comprehensive TTE. At the present time, with the current commercially available devices, the use of transcatether aortic valve implantation in the management of native pure AR is somewhat limited by suboptimal outcomes compared with its use in aortic stenosis. However, as newer devices tailored for native AR may become available, we do not anticipate a significant role of the classification as its primary design is to inform tailored surgical approaches for valve preservation and repair.

While not the focus of our case series, which highlights two-dimensional (2D) imaging, it must be acknowledged that three-dimensional imaging has several advantages in the assessment of AR mechanism primarily through permitting optimal alignment when assessing valve anatomy (number of cusps, presence of raphe, commissural orientation) and measuring cusp motion through parameters such as effective, geometric, and coaptation height.[11]

Increasingly patients are undergoing multiple modes of imaging that provide additional value in the assessment of AR. Cardiovascular magnetic resonance imaging has the ability to assess AR severity primarily through calculation of the regurgitant volume/fraction and the consequences of chronic AR on LV size, volumes, and function and has been shown to have incremental value that in many cases results in a reclassification of AR severity.[12] Cardiovascular magnetic resonance imaging is typically recommended when there is a discordance between the echocardiographic classification of AR severity and the suspected severity based on clinical assessment or the degree of LV enlargement.[8,13] Cardiovascular magnetic resonance imaging has also been demonstrated to have reasonable agreement with echocardiography in defining the mechanism of AR.[14] Similar to cardiovascular magnetic resonance imaging, cardiac computed tomography provides an accurate assessment of aortic dimensions and LV remodeling as well as aortic valve anatomy, which allows it to provide useful information in the assessment of patients with AR, although data on its use to define AR mechanism are lacking. We suggest that common nomenclature should be used when defining the mechanism(s) of AR across these various imaging modalities.

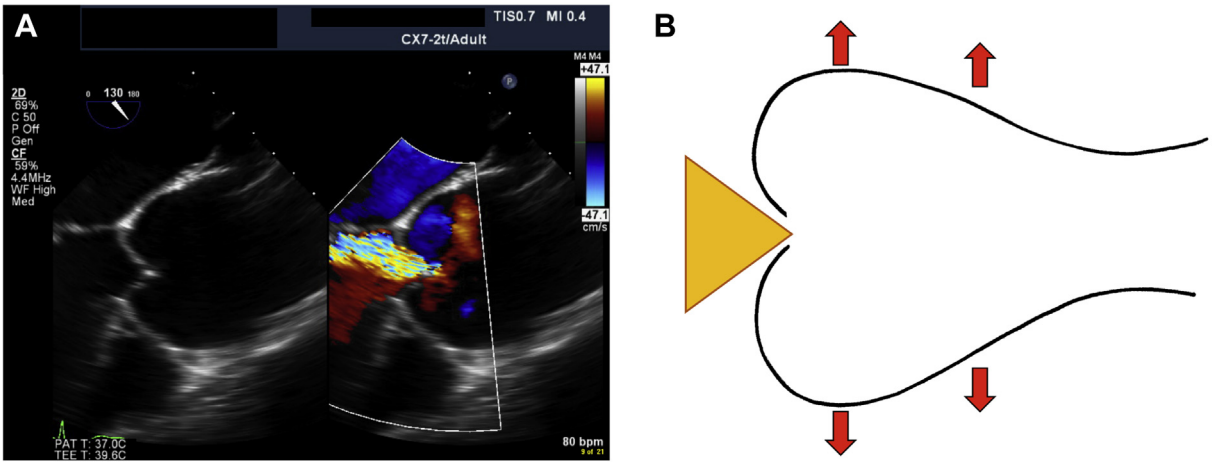

Figure 3 Type Ib AR. **(A)** Two-dimensional TEE midesophageal long-axis view, 130°, diastolic phase, without and with color demonstrating severe AR (Video 2). **(B)** Transesophageal echocardiographic long-axis view depiction showing aortic root (and STJ) enlargement with a central jet of AR.

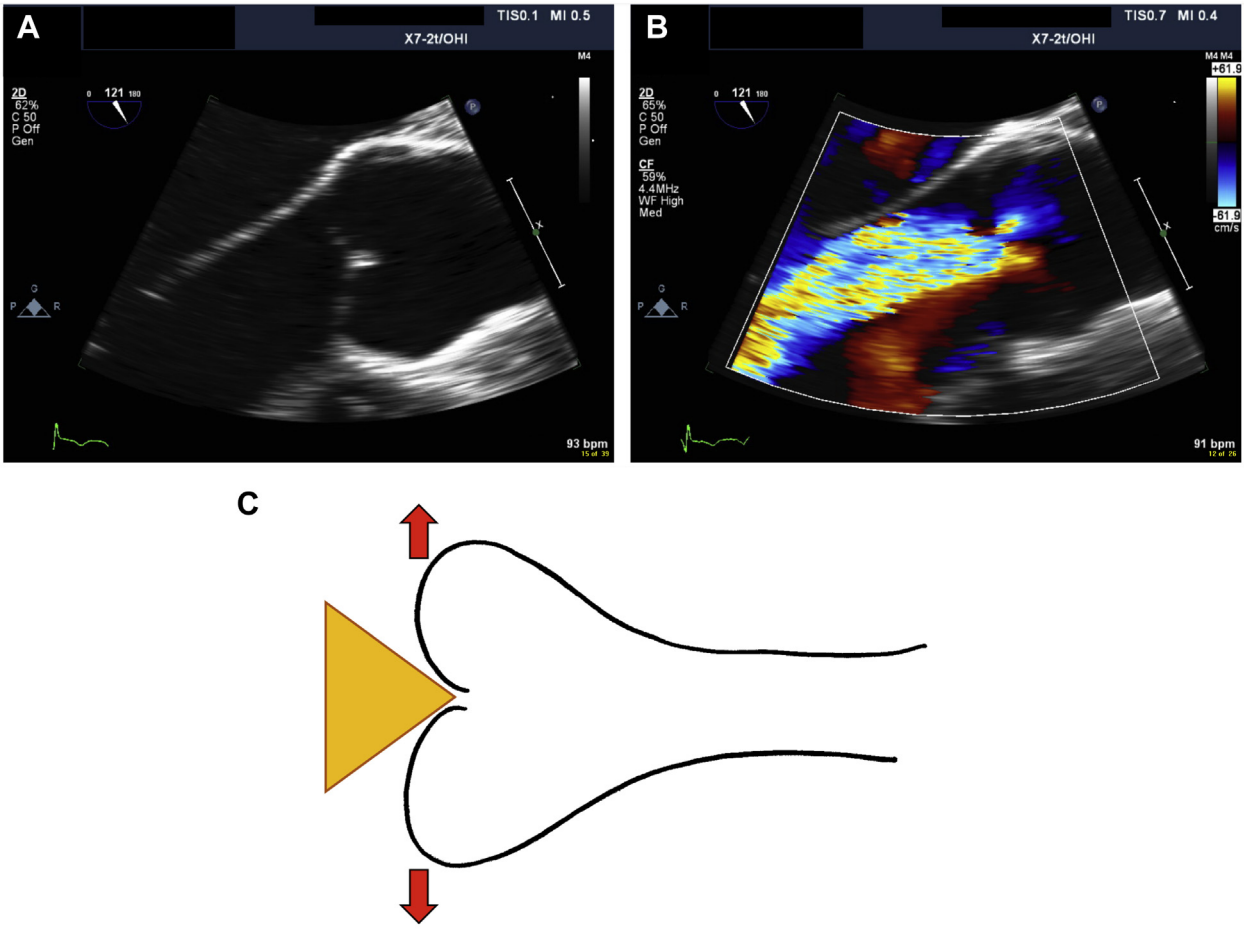

Figure 4 Type Ic AR. **(A, B)** Two-dimensional TEE midesophageal long-axis view, 121°, diastolic phase, without and with color Doppler, demonstrates severe AR (VCW 0.8 cm; Video 3). **(C)** Transesophageal echocardiographic long-axis view depiction showing isolated enlargement of the AoA with a central jet of AR.

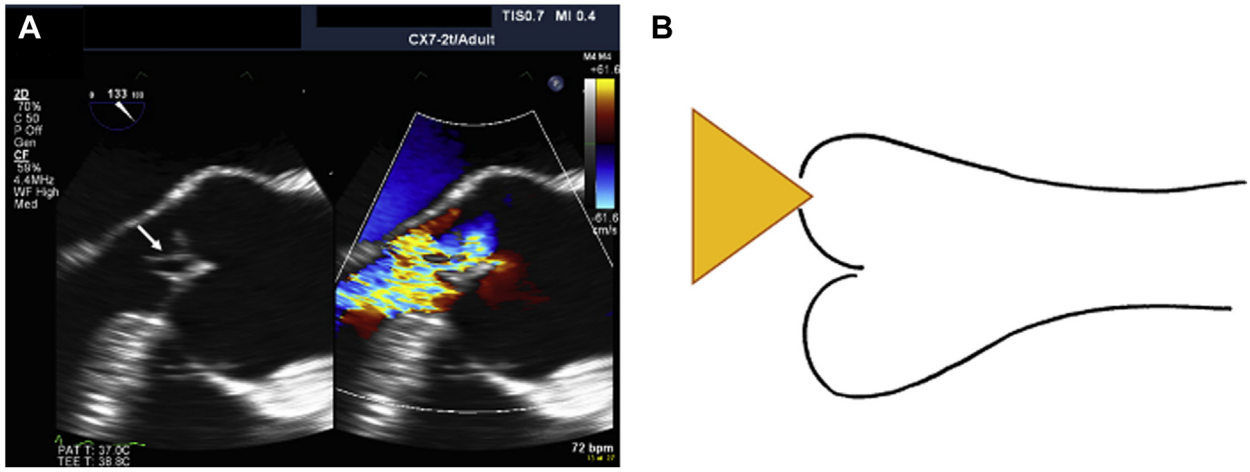

Figure 5 Type Id AR. **(A)** Two-dimensional TEE midesophageal long-axis view, 133° degrees, diastolic phase, without and with color Doppler, demonstrates two filamentous linear structures on the LV side of the AV leaflets (perforated diverticulum; *arrow*). With color Doppler, severe AR is demonstrated (VCW, 0.8 cm; Video 4). **(B)** Transesophageal echocardiographic long-axis view depiction showing that the jet originates in the body of the noncoronary cusp and not at the site of coaptation.

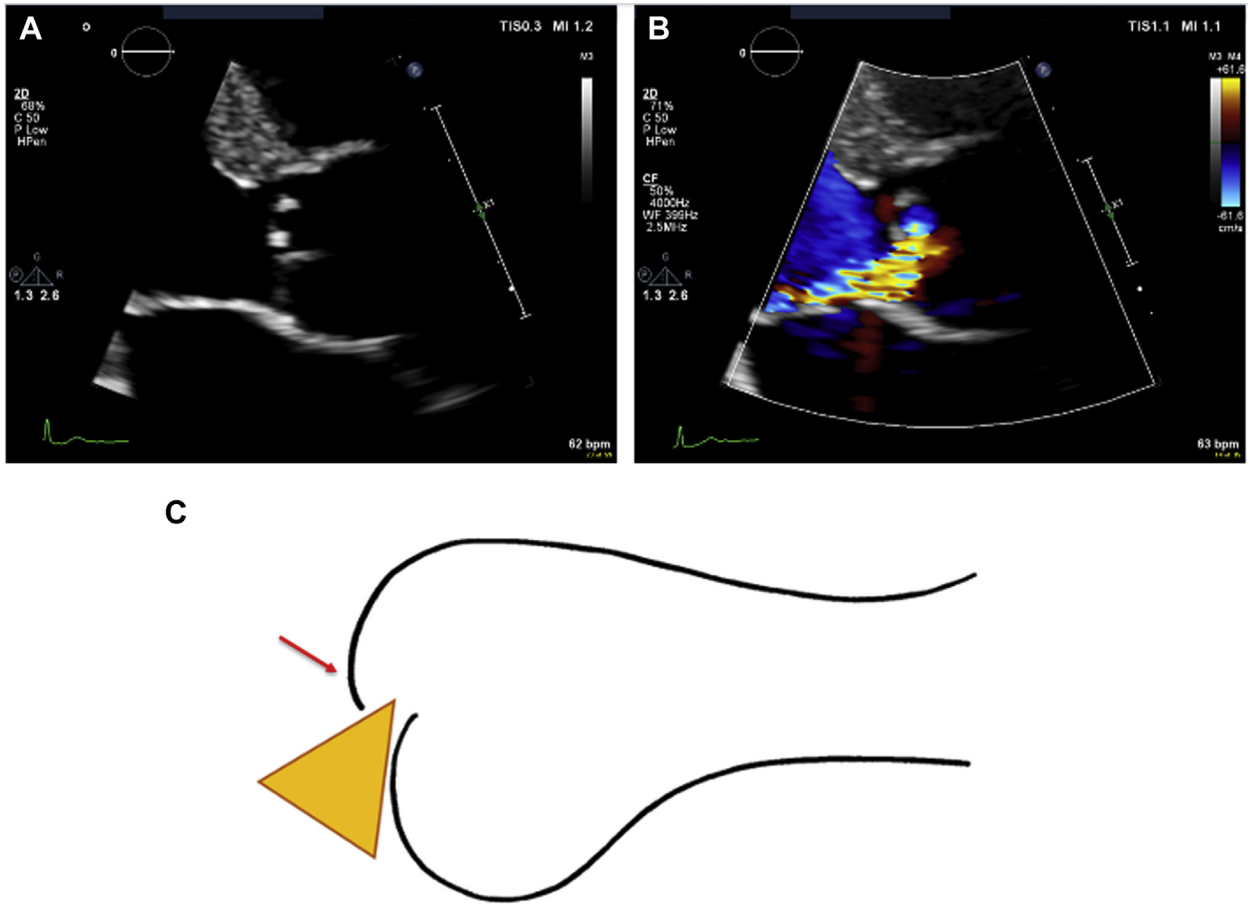

Figure 6 Type II AR. **(A, B)** Transthoracic echocardiographic parasternal long-axis, diastolic phase without and with color demonstrating an eccentric jet of severe AR directed toward the anterior mitral valve leaflet (Video 5). **(C)** Transthoracic echocardiographic long-axis view depiction showing right coronary cusp prolapse (*arrow*), resulting in an eccentric jet of AR.

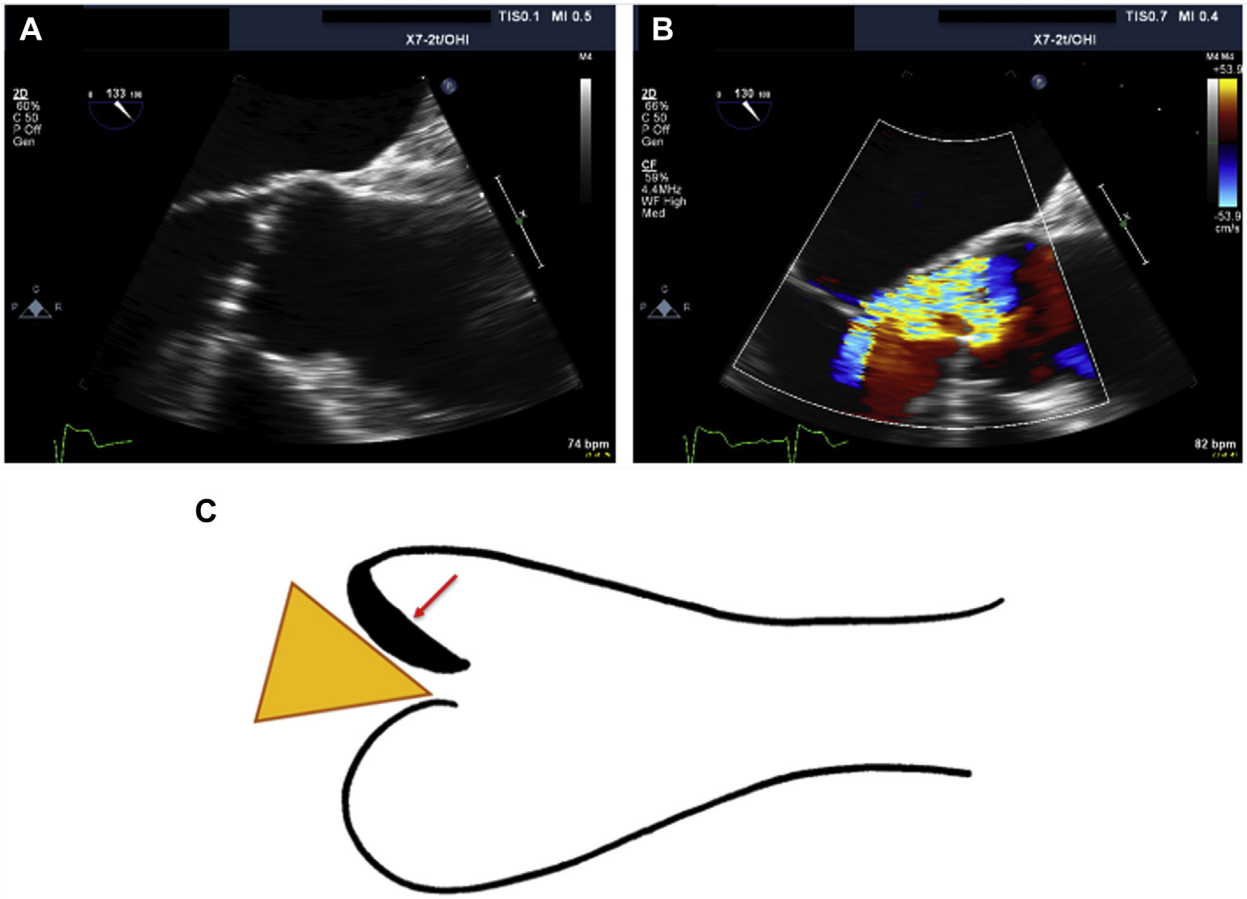

Figure 7 Type III AR. **(A, B)** Two-dimensional TEE midesophageal long-axis views, 130°, diastolic phase, without and with color Doppler showing an eccentric jet of severe AR directed toward the anterior mitral valve leaflet (Video 6). **(C)** Transesophageal echocardiographic long-axis view depiction showing asymmetric cusp degeneration resulting in noncoronary cusp restriction (*arrow*) and an eccentric jet of AR.

CONCLUSION

The mechanism of AR can be described using a functional classification that aligns with approaches to aortic valve repair. We believe that these definitions and a standardized approach as outlined through our case series can assist with uptake of a mechanism-based approach to AR for the echocardiographer and the multimodality imager.

SUPPLEMENTARY DATA

Supplementary data related to this article can be found at https://doi.org/10.1016/j.case.2022.03.004.

REFERENCES

1. Boodhwani M, de Kerchove L, Glineur D, Poncelet A, Rubay J, Astarci P, et al. Repair-oriented classification of aortic insufficiency: impact on surgical techniques and clinical outcomes. J Thorac Cardiovasc Surg 2009;137:286-94.
2. El Khoury G, Glineur D, Rubay J, Verhelst R, d'Udekem d'Acoz Y, Poncelet A, et al. Functional classification of aortic root/valve abnormalities and their correlation with etiologies and surgical procedures. Curr Opin Cardiol 2005;20:115-21.
3. Le Polain de Waroux JB, Pouleur AC, Goffinet C, Vancraeynest D, Van Dyck M, Robert A, et al. Functional anatomy of aortic regurgitation: accuracy, prediction of surgical repairability and outcome implications of transesopheal echocardiography. Circulation 2007;116(Suppl I):I264-9.
4. Vanoverschelde JL, van Dyck M, Gerber B, Vancraeynest D, Melchoir J, de Meester C, et al. The role of echocardiography in aortic valve repair. Ann Cardiothoac Surg 2013;2:65-72.
5. Piazza N, de Jaegere P, Schultz C, Becker AE, Serruys PW, Anderson RH. Anatomy of the aortic valvar complex and its implications for transcatheter implantation of the aortic valve. Circ Cardiovasc Interv 2008;1:74-81.
6. Lang RM, Badano LP, Mor-Avi V, Afilalo J, Armstrong A, Ernande L, et al. Recommendations for cardiac chamber quantification by echocardiography in adults: an update from the American Society of Echocardiography and the European Association of Cardiovascular Imaging. J Am Soc Echocardiogr 2015;28:1-39.
7. Isselbacher EM. Thoracic and abdominal aortic aneurysms. Circulation 2005;111:816-28.
8. Zoghbi WA, Adams D, Bonow RO, Enriquez-Sarano M, Foster E, Grayburn PA, et al. Recommendations for noninvasive evaluation of native valvular regurgitation: a report from the American Society of Echocardiography Developed in Collaboration with the Society for Cardiovascular Magnetic Resonance. J Am Soc Echocardiogr 2017;30:303-71.

9. Hahn RT, Saric M, Faletra FF, Garg R, Gillam LD, Horton K, et al. Recommended standards for the performance of transesophageal echocardiographic screening for structural heart intervention: from the American Society of Echocardiography. J Am Soc Echocardiogr 2022;35:1-76.
10. Yang LT, Michelena HI, Maleszewski JJ, Schaff HV, Pellikka PA. Contemporary etiologies, mechanisms, and surgical approaches in pure native aortic regurgitation. Mayo Clin Proc 2019;94:1158-70.
11. Berrebi A, Monin JL, Lansac E. Systematic echocardiographic assessment of aortic regurgitation: what should the surgeon know for aortic valve repair? Ann Cardiothorac Surg 2019;8:331-41.
12. Kammerlander AA, Wiesinger M, Duca F, Aschauer S, Binder C, Zotter Tufaro C, et al. Diagnostic and prognostic utility of cardiac magnetic resonance imaging in aortic regurgitation. JACC Cardiovasc Imaging 2019;12(8 Pt 1):1474-83.
13. Otto CM, Nishimura RA, Bonow RO, Carabello BA, Erwin JP, Gentile F, et al. 2020 ACC/AHA guideline for the management of patients with valvular heart disease: a report of the American College of Cardiology/American Heart Association Joint Committee on Clinical Practice Guidelines. J Am Coll Cardiol 2021;77:e25-197.
14. Richardson M, Raad N, Coisne A, Ridon H, Polge AS, Mouton S, et al. Assessment of aortic regurgitation mechanism with cardiac magnetic resonance: an echocardiography comparative study. Eur Heart J Cardiovasc Imaging 2021;22(Suppl 1):i81.